Гідроксид нікелю широко використовується в гібридних суперконденсаторах. Високу електрохімічну активність проявляє α-$Ni(OH)_2$, отриманий темплатним гомогеним осадженням. Можливим недоліком об'ємного темплатного синтезу є включення темплату в склад гідроксиду та відсутність даних щодо впливу його залишкової кількості. Для зниження залишкової кількості темплату запропоновано використати метод багатократної промивки. Також було проведено порівняльне вивчення впливу залишкової кількості темплату та використання існуючої кількості темплату без введення зовнішнього зв'язуючого. Для проведення дослідження були отримані зразки $Ni(OH)_2$ методом темплатного гомогенного осадження при використанні в якості темплату естеру целюлози Culminal C8465 з концентрацією 0,5 %. Структурні властивості зразків були вивчені методом рентгенофазового аналіза, розміри та морфологію частинок – методом скануючої електронної мікроскопії. Електрохімічні характеристики вивчались гальваностатичним зарядно-розрядним циклюванням намазного електрода, виготовленого як із застосуванням 3 % зв'язуючого, так і без введення зв'язуючого, в режимі суперконденсатора. Виявлено, що при використанні зовнішнього зв'язуючого питомі ємності зразка із високим залишковим вмістом темплату дуже низькі через блокування активної поверхні. При використанні цього зразка без введення зовнішнього зв'язуючого питома ємність підвищується в 1,8–18,4 рази. Зниження залишкової кількості темпалату при однократній промивці збільшило питомі ємності зразку в незначній мірі. Виявлено, що оптимальними є двух та трьохкратні промивки, при яких питомі ємності зразків збільшилися у 4,3–53,9 рази, до 490 Ф/г і 50,7 мА·год/г. Збільшення кількості промивок (і відповідно зниження залишкової кількості темплату) призводить до зниження питомих характеристик. Можливо це пояснюється наявністю оптимального вмісту, при якому врівноважується негативний вплив темплата із блокуванням питомої поверхні та позитивний вплив зі стабілізацією нанорозмірних часток гідроксиду. Висловлено рекомендацію експериментально визначати оптимальну кількість промивок для формування оптимального залишкового вмісту конкретного темплату

Ключові слова: гідроксид нікелю, темплатний синтез, гомогенне осадження, суперконденсатор, зв'язуюче, залишковий вміст

UDC 54.057:544.653:621.13:661.13
DOI: 10.15587/1729-4061.2019.181020

THE EFFECT OF TEMPLATE RESIDUAL CONTENT ON SUPERCAPACITIVE CHARACTERISTICS OF $Ni(OH)_2$, OBTAINED BY TEMPLATE HOMOGENEOUS PRECIPITATION

V. Kovalenko
PhD, Associate Professor
Department of Analytical Chemistry and Food Additives and Cosmetics*
E-mail: vadimchem@gmail.com
Senior Researcher**
V. Kotok
PhD, Associate Professor
Department of Processes, Apparatus and General Chemical Technology*
E-mail: valeriykotok@gmail.com
Senior Researcher**
*Ukrainian State University of Chemical Technology
Gagarina ave., 8, Dnipro, Ukraine, 49005
**Competence center "Ecological technologies and systems"
Vyatka State University
Moskovskaya str., 36, Kirov, Russian Federation, 610000

Received date 13.08.2019
Accepted date 03.10.2019
Published date 31.10.2019

1. Introduction

At the present time, supercapacitors (SC) are a modern type of chemical power sources (CPS). They are used for the starting of electric motors of, for instance, electromobiles and pump stations, as starter SPC for combustion engines. SC are also used in uninterruptible power supplies for computers, medical equipment, critical infrastructure facilities. Hybrid supercapacitors possesses the best characteristics, owing to their high charge and discharge rates. In the hybrid supercapacitor, the electrochemical reaction at the Faradaic electrode occurs on the surface and in a thin layer of particles of active material. Thus, there are special requirements to the active material of the Faradaic electrode, regarding specific surface area, crystal structure and electrochemical activity [1, 2]. The active material of the Faradaic electrode should be mainly composed of nano- and submicron-sized particles with a high specific surface area. Nickel hydroxide is widely used as an active material for the Faradaic electrode of supercapacitors. $Ni(OH)_2$ is used on its own [3], as nanosized [4] or ultrafine powder [5], and as a composite with nanocarbon material (graphene oxide [6], carbon nanotubes [7]).

Many methods have been developed for the synthesis of nickel hydroxide and nickel-based layered double hydroxides [8]. Among chemical precipitation methods there are direct chemical precipitation (slow addition of basic solution to a solution of Ni^{2+}) [9] or reversed synthesis (slow addition of nickel salt solution to basic solution) [10, 11], and also two-step high-temperature synthesis [12] or sol-gel method [13]. Electrochemical methods are also used for the synthesis of nickel hydroxides [14, 15], including synthesis in the slit diaphragm electrolyzer [16, 17].

Two structural modifications of nickel hydroxide have been described [18]. β-form (formula $Ni(OH)_2$, brucite-like

crystal structure) and α-form (formula $3Ni(OH)_2 \cdot 2H_2O$, hydrotalcite-like crystal structure). β-$Ni(OH)_2$ has high cycling stability and is widely used as an active material of accumulators and supercapacitors. α-$Ni(OH)_2$ has significantly higher electrochemical characteristics compared to β-$Ni(OH)_2$, and can be used in supercapacitors more effectively. Thus, the development and optimization of synthesis methods for the preparation of highly active α-$Ni(OH)_2$ are relevant problems.

2. Literature review and problem statement

Synthesis method and conditions directly define the micro- and macrostructure of particles, which determine the electrochemical activity of nickel hydroxide. For effective application in supercapacitors, nickel hydroxide should have specific properties [19], particularly, it should be α-$Ni(OH)_2$ with optimal crystallinity and consist of submicron [5] and nanoscale [4, 20] particles.

During the formation of nickel hydroxide, the nucleation rate is significantly higher than the rate of crystal growth. Because of that, $Ni(OH)_2$ is formed according to a two-stage mechanism [21]: very fast first stage – formation of the initial amorphous particle; slow second stage – crystallization (aging) of the initial particle. This results in the formation of hydrophilic precipitate that contains a large amount of mother liquor. During filtering (especially under vacuum), the precipitate particles are pressed and caked during the following drying, which leads to a significant increase in particle size and decrease of their specific surface area. Two approaches can be used to prevent that:

1) use of synthesis method with low nucleation rate and very high rate of crystal growth;

2) addition of special compounds that would prevent the merging of initial particles.

The first approach can be realized by means of homogeneous precipitation [22]. The principle of this method is the formation of OH^- ions in the entire volume of reaction solution as a result of the thermal hydrolysis of ammine compounds (urea [23, 24], hexamethylenetetramine [25]). Homogeneous precipitation can be conducted in aqueous solutions and mixed solvents [26] or non-aqueous solutions like ionic liquids [27]. For the preparation of ultrafine or nano-sized $Ni(OH)_2$, homogeneous precipitation should be conducted at elevated temperatures up to 150–180 °C. Мiкrowave heating is employed for the same reason [28].

The second approach is realized by the application of surfactants [29, 30] or templates. The latter is so-called template synthesis, i. e. synthesis of the compound inside the matrix (template). This method is usually applied for the formation of coatings such as electrochromic $Ni(OH)_2$ films [31], tripolyphosphate coatings [32] or direct formation of the Faradaic electrode on the nickel foam surface [33]. This results in the formation of composite materials similar to polymer composites [34]. It should be mentioned that in this case, there is no need to remove the template. The paper [35] describes the application of water-soluble templates for the synthesis of nickel hydroxide.

However, the most promising route is the combination of both approaches – the use of template homogeneous precipitation. It should be noted that such a combined method of template homogeneous precipitation hasn't been studied in detail. Template for the synthesis of $Ni(OH)_2$ in aqueous solution should correspond to specific requirements – be water-soluble, have affinity to nickel compounds and form a 3D matrix in solution. PEG6000 is used as a water-soluble template [36]. Polyvinyl alcohol (PVA) is also a promising template. PVA is used as a porosity-controlling agent in the synthesis of mesoporous alumina oxide [37], hydroxyapatite crystals (along with sodium dodecyl sulfate) [38]. PVA is also used for the synthesis of MFI zeolite [39]; MgO for dye removal from wastewater [40], formation of single-layer [41, 42] and multilayer [43] hydroxide films, preparation of 3D-structured macroporous oxides and hierarchic zeolites [44], as well as for improving the adhesion of coatings on the ITO surface [45]. The paper [46] describes the high effectiveness of cellulose ether Culminal C8465 as a template.

However, template synthesis has a significant disadvantage. After synthesis, it is of importance to remove the template. Difficulties with template removal lead to the whole template-free direction for the preparation of ultrafine systems, such as calcium titanate [47] and zeolite ZSM-5 [48]. The paper [49, 50] describes the method for template-free synthesis of nanosized $Ni(OH)_2$. For supercapacitor applications, the presence of the template in the active material can lead to partial blocking of the material surface, template oxidation, and other side-effects. From this point of view, it is of most importance to remove as much template as possible from active material, particularly from $Ni(OH)_2$. Different methods are used to remove surfactants and templates, including ozone oxidation [51]. However, when preparing the pasted supercapacitor electrode, a binder is added to the active mass [29] to prevent it from falling off from the current collector. However, the binder is an inert component of the active mass, which lowers its specific characteristics. The paper [52] describes a negative effect of high amounts of template residue on supercapacitive properties of $Ni(OH)_2$. So, the template should be removed or employed as a binder during the preparation of the pasted electrode (this possibility is described in [53]).

However, the conducted analysis did not reveal any information on the level of template residue at which a negative impact on electrochemical properties of nickel hydroxide is minimal. Additionally, there is promise in comparing electrochemical properties of $Ni(OH)_2$ samples when removing the template and using it as a binder. Conducting study in this direction becomes necessary for finding the optimal characteristics of active materials to be used in supercapacitors.

3. The aim and objectives of the study

The aim of the work is to study the electrochemical characteristics of nickel hydroxide with different amounts of template residue to obtain highly active supercapacitive $Ni(OH)_2$.

To achieve the set aim, the following objectives were formulated:

– to synthesize nickel hydroxide samples via homogeneous precipitation with high template concentration, remove the template residue through multiple rinsing;

– to use the prepared $Ni(OH)_2$ samples with different levels of template residue (different number of rinsing stages) for preparing pasted supercapacitor electrodes and studying their electrochemical characteristics;

– to use a comparative analysis of electrochemical characteristics to determine the optimal number of rinsing stages for the preparation of highly active nickel hydroxide and determine the effectiveness of residual template in $Ni(OH)_2$ as an inner binder for the preparation of pasted electrode compared to the removal of excess template.

4. Materials and methods for synthesis and analysis of nickel hydroxide samples

4. 1. Preparation of main nickel hydroxide sample

For the synthesis of the reference $Ni(OH)_2$ sample, homogeneous precipitation was employed, in which precipitation from nickel nitrate solution was induced by thermal hydrolysis of urea in the presence of high molecular weight water-soluble template Culminal C8465 with the concentration of 0.5 % (wt.) according to the method described in [53]. The amount of residual template was lowered through multistage rinsing (1, 2, 3 and 4 times). On each rinsing stage, the samples were soaked in 1,000 ml of distilled water for a day, filtered and dried. The samples were labeled as follows: **0.5-R-3**, where 0.5 – template concentration (0.5 % wt.), R – indicates rinsing; 3 – number of rinsing stages. The sample **0.5-R-0** – reference, no rinsing.

4. 2. Characterization of nickel hydroxide samples

The crystal structure of the samples was studied by means of X-ray diffraction analysis (XRD) using DRON-3 diffractometer (Russia) (Co-Kα, radiation, scan range 10–90° 2θ, scan rate 0.1°/s).

The shape and size of the particles were studied using scanning electron microscope 106 – I (SELMI, Ukraine).

Electrochemical properties of nickel hydroxides were evaluated by means of galvanostatic charge-discharge cycling in special cell YSE (USSR) using digital potentiostat Ellins P-8 (Russia). The working electrode was prepared by pasting a mixture of nickel hydroxide (81 % wt.), graphite (16 % wt.) and PTFE as a binder (3 % wt. in terms of dry matter) [53] on nickel foam current collector [54]. To compare the effectiveness of template removal and its usability as an inner binder, an electrode was prepared without introducing additional binders to the active mass. The sample was labeled as **0.5-R-0BF** (BF – binder-free). Electrolyte – 6M KOH. Counter electrode – nickel mesh, reference electrode – Ag/AgCl (KCl sat.). Charge-discharge cycling was conducted in the supercapacitor regime at current densities of 20, 40, 80 and 120 mA/cm^2 (5 cycles at each current density). Discharge curves were used to calculate specific capacities C_{spec} (F/g) and Q_{spec} with discharge to 0 V and full discharge.

5. Results of studying characteristics of nickel hydroxide samples synthesized with different contents of residual template

The results of XRD analysis (Fig. 1) reveal that the nickel hydroxide sample before multistage rinsing is α-$Ni(OH)_2$ with low crystallinity.

Fig. 2 shows SEM images of unwashed **(0.5-R-0)** and 4 times washed **(0.5-R-4)** samples. It is noted that upon removal of the template (higher number of rinsing stages), breakdown of particle agglomerates occurs, decreasing their size.

Fig. 3–6 show charge and discharge curves of different samples plotted as capacities.

The charge-discharge curves reveal that when an external binder is used, the unwashed sample **0.5-R-0** (Fig. 3) has very low specific capacities. Multistage rinsing results in lower template content and higher specific capacities of the samples in the series "sample **0.5-R-0** (Fig. 3) – sample **0.5-R-2** (Fig. 5) – sample **0.5-R-4** (Fig. 6)". When the external binder wasn't introduced (sample **0.5-R-0BF,** Fig. 4), the specific capacity increased by two times. However, washed samples (with low binder content) have significantly higher capacities, despite the addition of external binder to the active mass.

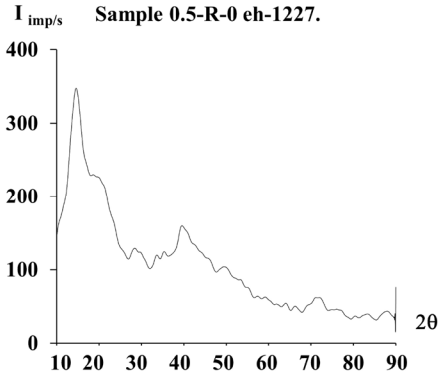

Fig. 1. XRD pattern of nickel hydroxide samples **0.5-R-0**

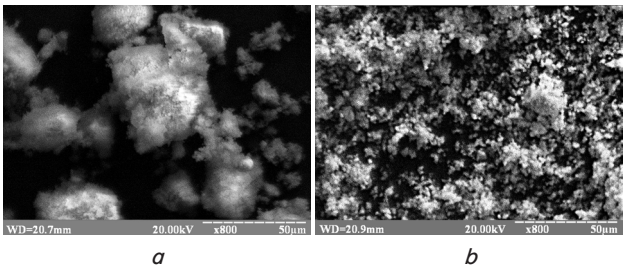

a *b*

Fig. 2. SEM images of nickel hydroxide samples: *a* – **0.5-R-0**; *b* – **0.5-R-4**

Fig. 7, 8 show data on specific capacities of the samples in different charge-discharge cycling regimes.

In general, it should be noted that for all samples, an increase of current density leads to an increase in specific capacities. Another thing to note is that the sample **0.5-R-0**, which wasn't washed from the residual template and was introduced into the active mass using the external binder, at 20 mA/cm^2 demonstrated a very low specific capacity of 7.2 F/g (discharge to E=0 B) and 0.7 mA·h/g (full discharge). With an increase of current density to 120 mA/cm^2, specific capacities increased insignificantly. The discharge curves of this sample (Fig. 3) are sloped without pronounced plateaus, capacity increases with each subsequent cycle. Without an external binder, the sample **0.5-R-0BF** demonstrated higher specific capacities, reaching 231–244 F/g at 80 and 120 mA/cm^2. A decrease of template residue content (upon rinsing) significantly increased the specific capacities of the samples. However, subsequent one-, two- and four-stage rinsing had an insignificant effect on electrochemical activity. In the series "sample **0.5-R-1** – sample **0.5-R-2** – sample **0.5-R-3** – sample **0.5-R-4**", maximum specific capacities are demonstrated by the samples **0.5-R-2** and **0.5-R-3**. Thus, after double and triple rinsing, the content of residual template decreased and specific capacities of nickel hydroxide samples increases. However, further rinsing (further decrease of template content) leads to some decrease of specific capacities, especially at lower cycling current densities. It should be noted that the specific capacity of the sample **0.5-R-0BF** obtained from pasted electrode without external binder turned out to be lower after multistage rinsing **(0.5-R-1, 0.5-R-2, 0.5-R-3, 0.5-R-4)**, obtained from the electrode with 3 % PTFE as a binder. The maximum achieved specific capacities were 490 F/g (discharge to E=0 B) and 292 F/g (full discharge) at 120 mA/cm^2 (sample **0.5-R-3** – triple rinsing). These values are comparable to the world's best samples [4, 5, 24].

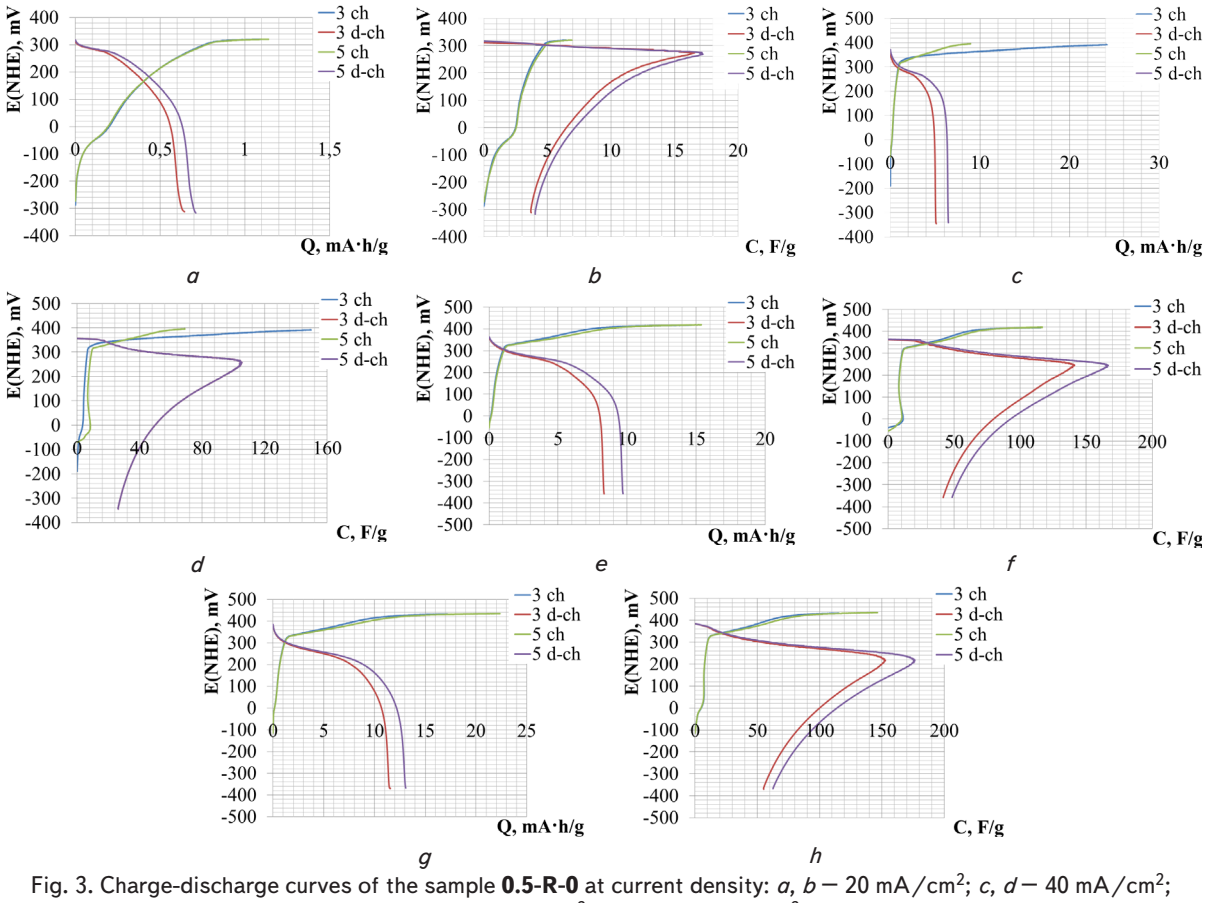

Fig. 3. Charge-discharge curves of the sample **0.5-R-0** at current density: *a*, *b* – 20 mA/cm^2; *c*, *d* – 40 mA/cm^2; *e*, *f* – 80 mA/cm^2; *g*, *h* – 120 mA/cm^2

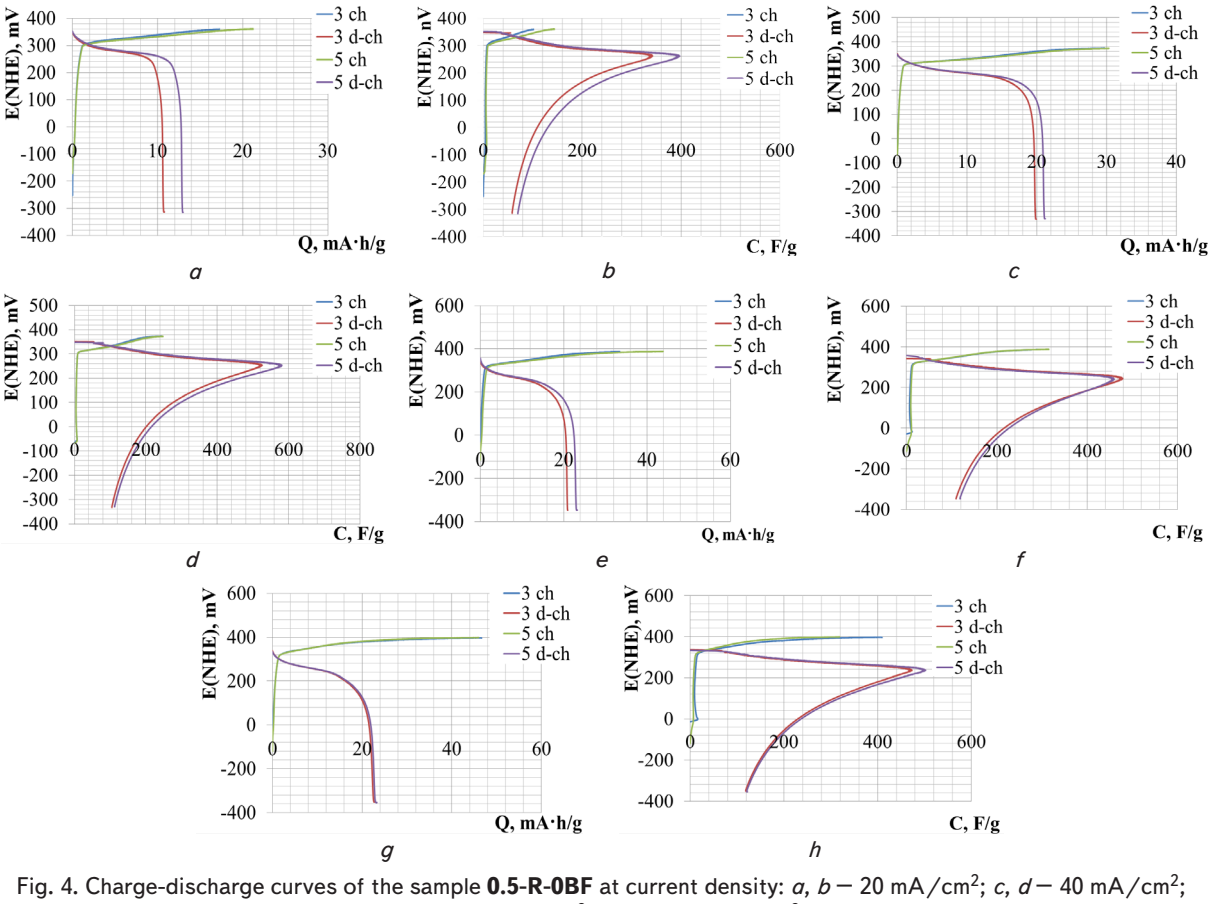

Fig. 4. Charge-discharge curves of the sample **0.5-R-0BF** at current density: *a*, *b* – 20 mA/cm^2; *c*, *d* – 40 mA/cm^2; *e*, *f* – 80 mA/cm^2; *g*, *h* – 120 mA/cm^2

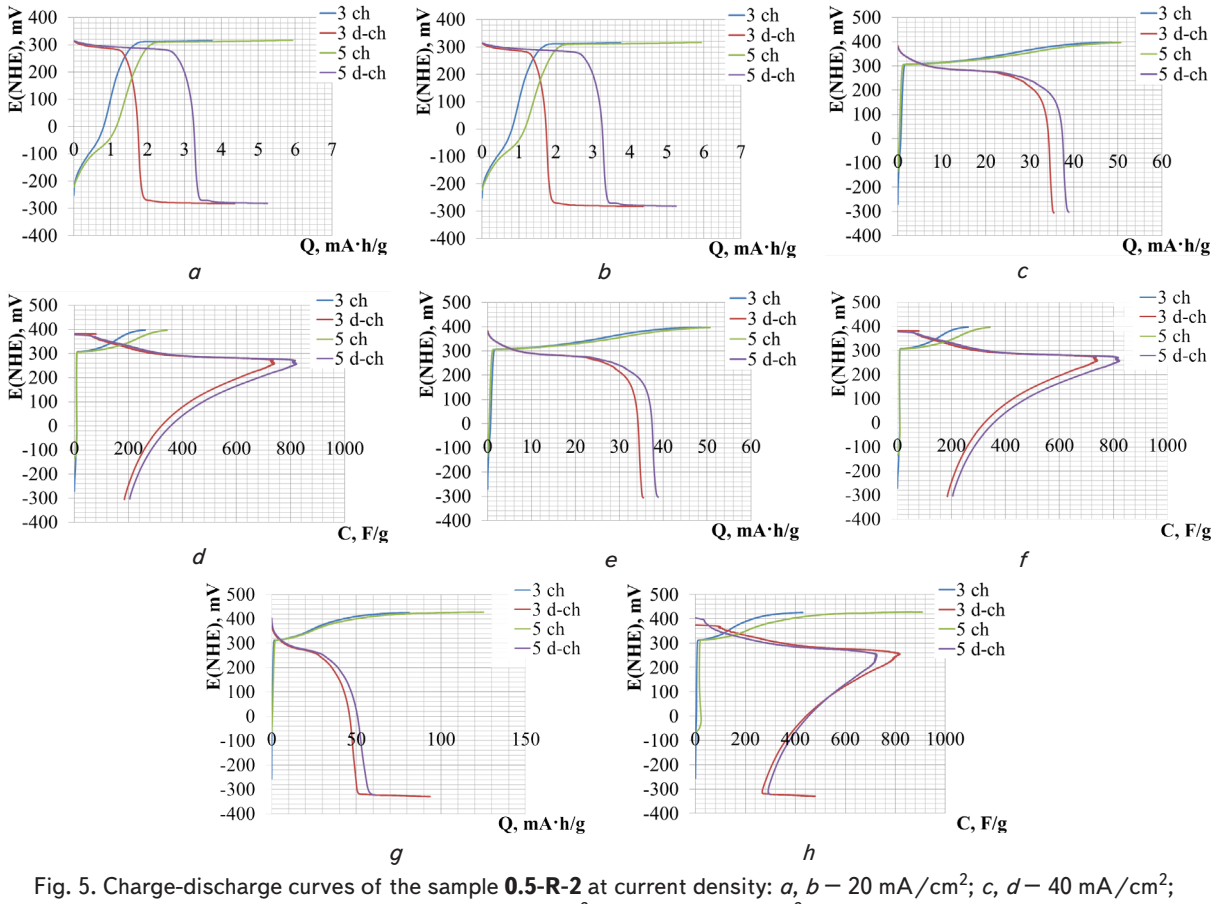

Fig. 5. Charge-discharge curves of the sample **0.5-R-2** at current density: *a*, *b* – 20 mA/cm^2; *c*, *d* – 40 mA/cm^2; *e*, *f* – 80 mA/cm^2; *g*, *h* – 120 mA/cm^2

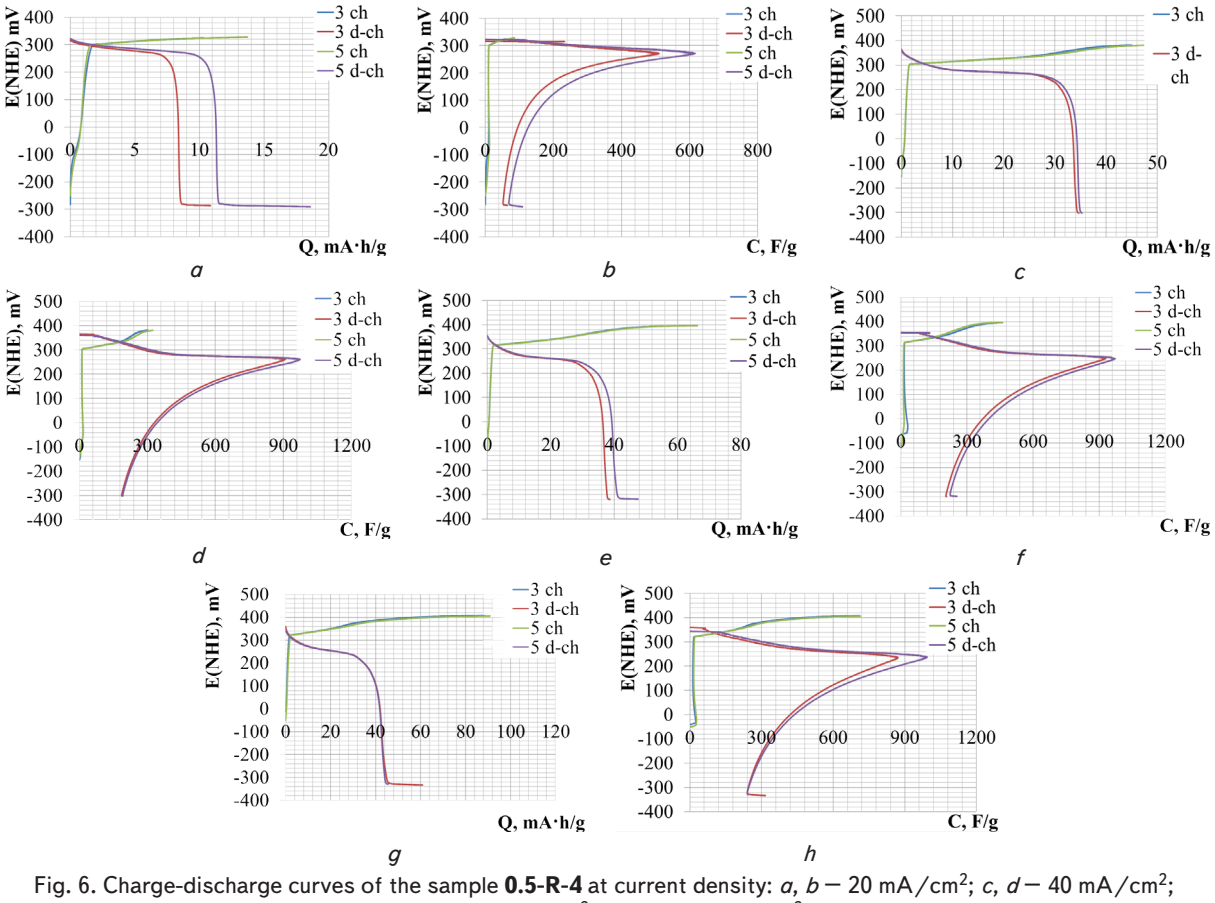

Fig. 6. Charge-discharge curves of the sample **0.5-R-4** at current density: *a*, *b* – 20 mA/cm^2; *c*, *d* – 40 mA/cm^2; *e*, *f* – 80 mA/cm^2; *g*, *h* – 120 mA/cm^2

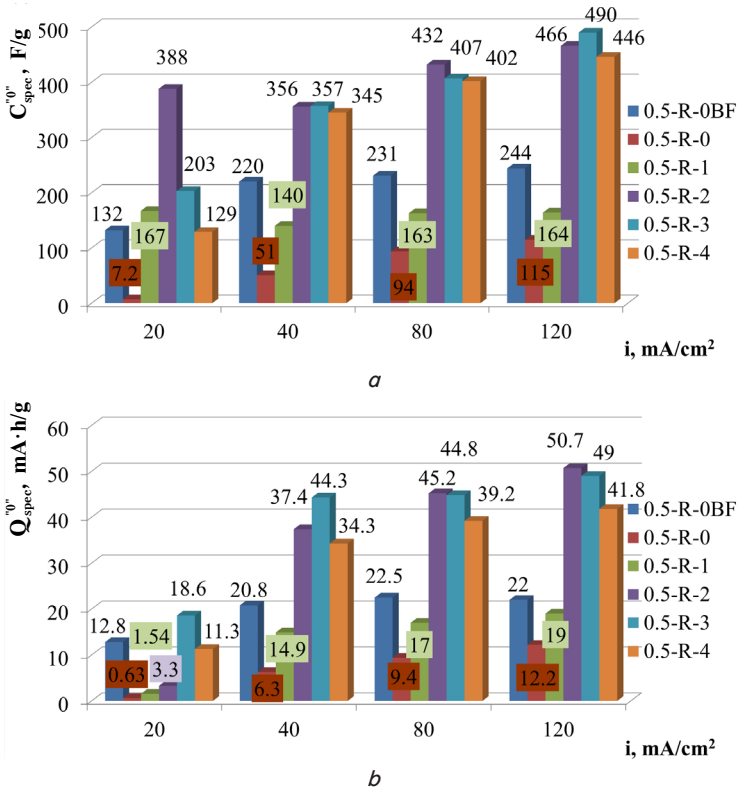

Fig. 7. Specific capacity of nickel hydroxide samples in galvanostatic charge-discharge cycling (discharge to E=0 B); a – C_{spec}, F/g; b – Q_{spec}, mA·h/g

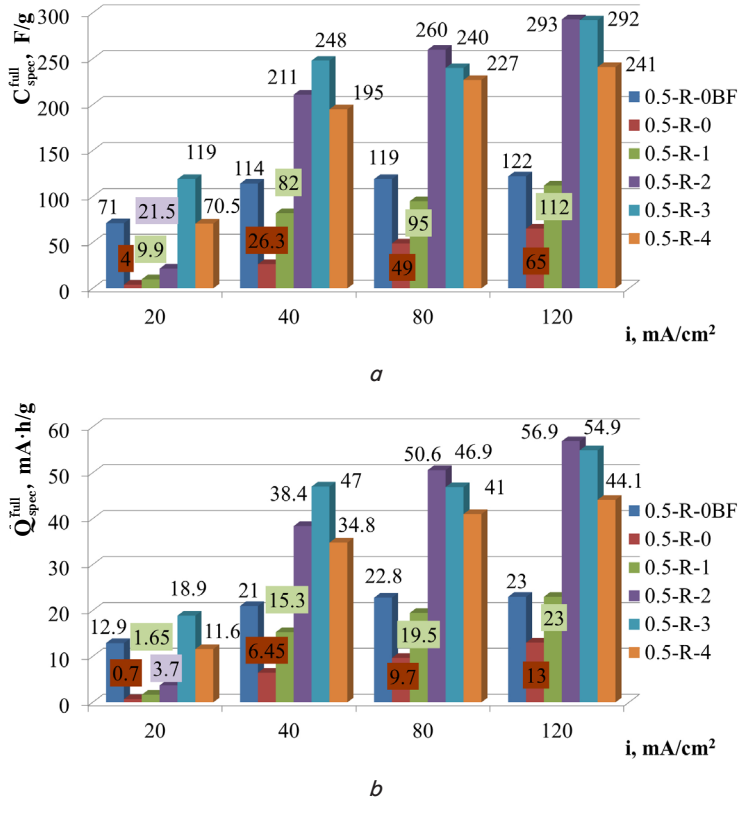

Fig. 8. Specific capacity of nickel hydroxide samples in galvanostatic charge-discharge cycling (full discharge); a – C_{spec}, F/g; b – Q_{spec}, mA·h/g

6. Discussion of studying characteristics of nickel hydroxide samples with different contents of residual template

Influence of residual template on characteristics of nickel hydroxide samples. The XRD pattern presented in Fig. 1 revealed that the sample is α-$Ni(OH)_2$. SEM images (Fig. 2, *a*) revealed the formation of particle aggregates when 0.5 % Culminal C8465 (sample **0.5-R-0**) was used as a template. As a template, Culminal C8465, in addition to forming the 3D matrix, likely interacts with synthesized hydroxide and expresses binding properties causing particle aggregation, especially at high concentration, which is in agreement with literature data [53].

Combined influence of template residue and external binder on the specific capacity of samples. The sample **0.5-R-0** (in pasted electrode with 3 % PTFE as an external binder) demonstrated rather low capacities at a current density of 20 mA/cm² 7.2 F/g (discharge to E=0 B) and 0.7 mA·h/g (full discharge). With an increase of current density to 120 mA/cm², specific capacities increased insignificantly. Such low specific characteristics indicate that the combined effect of residual template and external binder is negative, due to the blocking of the active surface of submicron hydroxide particles. This conclusion is in agreement with the characteristics of the sample **0.5-R-0BF**, which was used in the pasted electrode with the addition of external binder. At 20 mA/cm², the specific capacity of **0.5-R-0BF** exceeded the specific capacity of the sample **0.5-R-0** by 18.3–18.4 times (132 F/g and 12.9 mA·h/g, in comparison to 7.2 F/g and 0.7 mA·h/g). With an increase of cycling current density to 120 mA/cm², the specific capacitances increase due to the breakdown of particle agglomerates. The capacity ratio of the sample **0.5-R-0BF** and **0.5-R-0** decreased to 1.7–1.8 times. The discharge curves of the sample **0.5-R-0BF** (Fig. 4) have a more pronounced discharge plateau and higher charge-discharge stability.

Influence of the number of rinsing stages and content of template residue on characteristics of samples. SEM images revealed a sharp particle size decrease after 4-stage rinsing (sample **0.5-R-4**, Fig. 2, *b*) in comparison to the unwashed sample (**0.5-R-0**, Fig. 2, *a*). Multistage rinsing results in a decrease of template residue. The paper [53] states that the Culminal C8465 template has binding properties. Therefore, a decrease in the template content by rinsing should result in lower binding properties and breakdown of hydroxide particle agglomerates after synthesis and decrease of particle size, which is supported by SEM images.

One-stage rinsing (sample **0.5-R-1**) increased the specific capacities, but the effect of one-stage rinsing turned out to be lower than not using an external binder. Two- and three-stage rinsing increases the specific capacities significantly more, the specific capacities reached their maximum value (Table 1). This is explained by lesser block-

age of active surface and even its increase due to the breakdown of particle agglomerates.

Table 1

Maximum specific capacities of nickel hydroxide samples

i, mA/cm^2	20	40	80	120
C_{spec}^{max}, F/g	388	357	432	490
$C_{spec}^{max} / C_{spec}$, **(0.5-R-0)**	53.9	7	4.6	4.3
Sample	**0.5-R-2**	**0.5-R-2 0.5-R-3**	**0.5-R-2**	**0.5-R-2**
Q_{spec}^{max}, mA·h/g	18.6	44.3	45.2	50.7
$Q_{spec}^{max} / Q_{spec}$, **(0.5-R-0)**	25.6	6.9	4.7	3.9
Sample	**0.5-R-3**	**0.5-R-3**	**0.5-R-2**	**0.5-R-3**

According to Table 1, the maximum increase of specific capacity is observed at a low current density of 20 mA/cm^2. The increase of current density results in working through samples due to the breakdown of agglomerates formed by residual template. The agglomerate breakdown is more pronounced for the unwashed sample **0.5-R-0.**

Following the found tendency for one-, two- and three-stage rinsing, four-stage rinsing should further improve the specific capacity of the sample due to more complete removal of residual template. However, the specific capacities of the sample **0.5-R-4** (four-stage rinsing) decreased in comparison to the sample **0.5-R-3**. This result can be explained by the fact that initially formed particles are nano-sized, which is confirmed by the need for ultrafiltration membranes to filter this sample. These initial particles combine into agglomerates (groups of particles combined into one) and are stabilized by template residue. Excessive removal of the template likely caused particles to stick to each other, thus lowering the active surface area.

The found optimal number of rinsing stages allows to further improve the technology of template synthesis of nickel hydroxide and the characteristic of the obtained product by introducing the rinsing stage.

In summary, it can be said that the found influence of template residue is specific for Culminal C8465, which possesses significant binding properties. Other templates can have different properties towards synthesized compounds, as was experimentally found for polyvinyl alcohol [52]. Therefore, the number of rinsing stages should be established experimentally for each template.

7. Conclusions

1. The influence of Culminal C8465 template residue on the characteristics of nickel hydroxide samples prepared by homogeneous precipitation in the presence of 0.5 % wt. template was studied. The content of template residue was decreased by multiple rinsing. It was found that single rinsing increases the specific capacities of nickel hydroxide. The maximum values of specific capacities are characteristic for the samples after two- and three-stage rinsing (490 F/g and 50.7 mA·h/g). The increase of electrochemical activity is explained by lesser blockage of the active surface at lower content of template residue. A decrease of specific characteristics was found when the template content was decreased further with four-stage rinsing. This is due to the aggregation of initially formed particles at the low content of template residue.

2. Comparative analysis was conducted for the influence of decreasing the content of template residue upon rinsing (using an external binder in the active mass) and use of residual template as an inner binder without the use of external binder in the active mass. It was found that the unwashed sample in the active mass without an external binder increases its capacity by 1.8–18.4 times in comparison to unwashed samples in the active mass with 3 % of binder. However, the decrease of residual template after two-stage rinsing led to an increase of the sample's specific capacity by 4.3–53.9 times (with 3 % of binder in the active mass). Thus, the optimal number of rinsing stages that results in the optimal content of template residue, which stabilizes the aggregates of nanosized nickel hydroxide particles, resulting in high specific capacities, was found for the Culminal C8465 template. An opinion was expressed regarding the necessity of experimentally establishing the optimal number of rinsing stages to form the optimal content of template residue for a specific template.

References

1. Simon, P., Gogotsi, Y. (2008). Materials for electrochemical capacitors. Nature Materials, 7 (11), 845–854. doi: https://doi.org/10.1038/nmat2297
2. Burke, A. (2007). R&D considerations for the performance and application of electrochemical capacitors. Electrochimica Acta, 53 (3), 1083–1091. doi: https://doi.org/10.1016/j.electacta.2007.01.011
3. Lang, J.-W., Kong, L.-B., Liu, M., Luo, Y.-C., Kang, L. (2009). Asymmetric supercapacitors based on stabilized α-Ni(OH)$_2$ and activated carbon. Journal of Solid State Electrochemistry, 14 (8), 1533–1539. doi: https://doi.org/10.1007/s10008-009-0984-1
4. Lang, J.-W., Kong, L.-B., Wu, W.-J., Liu, M., Luo, Y.-C., Kang, L. (2008). A facile approach to the preparation of loose-packed Ni(OH)$_2$ nanoflake materials for electrochemical capacitors. Journal of Solid State Electrochemistry, 13 (2), 333–340. doi: https://doi.org/10.1007/s10008-008-0560-0
5. Aghazadeh, M., Ghaemi, M., Sabour, B., Dalvand, S. (2014). Electrochemical preparation of α-Ni(OH)$_2$ ultrafine nanoparticles for high-performance supercapacitors. Journal of Solid State Electrochemistry, 18 (6), 1569–1584. doi: https://doi.org/10.1007/s10008-014-2381-7
6. Zheng, C., Liu, X., Chen, Z., Wu, Z., Fang, D. (2014). Excellent supercapacitive performance of a reduced graphene oxide/Ni(OH)$_2$ composite synthesized by a facile hydrothermal route. Journal of Central South University, 21 (7), 2596–2603. doi: https://doi.org/10.1007/s11771-014-2218-7
7. Wang, B., Williams, G. R., Chang, Z., Jiang, M., Liu, J., Lei, X., Sun, X. (2014). Hierarchical NiAl Layered Double Hydroxide/Multiwalled Carbon Nanotube/Nickel Foam Electrodes with Excellent Pseudocapacitive Properties. ACS Applied Materials & Interfaces, 6 (18), 16304–16311. doi: https://doi.org/10.1021/am504530e

8. Hall, D. S., Lockwood, D. J., Bock, C., MacDougall, B. R. (2015). Nickel hydroxides and related materials: a review of their structures, synthesis and properties. Proceedings of the Royal Society A: Mathematical, Physical and Engineering Sciences, 471 (2174), 20140792. doi: https://doi.org/10.1098/rspa.2014.0792
9. Solovov, V., Kovalenko, V., Nikolenko, N., Kotok, V., Vlasova, E. (2017). Influence of temperature on the characteristics of Ni(II), Ti(IV) layered double hydroxides synthesised by different methods. Eastern-European Journal of Enterprise Technologies, 1 (6 (85)), 16–22. doi: https://doi.org/10.15587/1729-4061.2017.90873
10. Liu, C., Huang, L., Li, Y., Sun, D. (2009). Synthesis and electrochemical performance of amorphous nickel hydroxide codoped with Fe3+ and CO 3 2−. Ionics, 16 (3), 215–219. doi: https://doi.org/10.1007/s11581-009-0383-8
11. Li, J., Luo, F., Tian, X., Lei, Y., Yuan, H., Xiao, D. (2013). A facile approach to synthesis coral-like nanoporous β-Ni(OH)$_2$ and its supercapacitor application. Journal of Power Sources, 243, 721–727. doi: https://doi.org/10.1016/j.jpowsour.2013.05.172
12. Kovalenko, V. L., Kotok, V. A., Sykchin, A. A., Mudryi, I. A., Ananchenko, B. A., Burkov, A. A. et. al. (2016). Nickel hydroxide obtained by high-temperature two-step synthesis as an effective material for supercapacitor applications. Journal of Solid State Electrochemistry, 21 (3), 683–691. doi: https://doi.org/10.1007/s10008-016-3405-2
13. Xiao-yan, G., Jian-cheng, D. (2007). Preparation and electrochemical performance of nano-scale nickel hydroxide with different shapes. Materials Letters, 61 (3), 621–625. doi: https://doi.org/10.1016/j.matlet.2006.05.026
14. Tizfahm, J., Safibonab, B., Aghazadeh, M., Majdabadi, A., Sabour, B., Dalvand, S. (2014). Supercapacitive behavior of β-Ni(OH)$_2$ nanospheres prepared by a facile electrochemical method. Colloids and Surfaces A: Physicochemical and Engineering Aspects, 443, 544–551. doi: https://doi.org/10.1016/j.colsurfa.2013.12.024
15. Aghazadeh, M., Golikand, A. N., Ghaemi, M. (2011). Synthesis, characterization, and electrochemical properties of ultrafine β-Ni(OH)$_2$ nanoparticles. International Journal of Hydrogen Energy, 36 (14), 8674–8679. doi: https://doi.org/10.1016/j.ijhydene.2011.03.144
16. Kovalenko, V., Kotok, V. (2017). Obtaining of Ni-Al layered double hydroxide by slit diaphragm electrolyzer. Eastern-European Journal of Enterprise Technologies, 2 (6 (86)), 11–17. doi: https://doi.org/10.15587/1729-4061.2017.95699
17. Kovalenko, V., Kotok, V. (2018). Comparative investigation of electrochemically synthesized (α+β) layered nickel hydroxide with mixture of α-Ni(OH)$_2$ and β-Ni(OH)$_2$. Eastern-European Journal of Enterprise Technologies, 2 (6 (92)), 16–22. doi: https://doi.org/10.15587/1729-4061.2018.125886
18. Hall, D. S., Lockwood, D. J., Poirier, S., Bock, C., MacDougall, B. R. (2012). Raman and Infrared Spectroscopy of α and β Phases of Thin Nickel Hydroxide Films Electrochemically Formed on Nickel. The Journal of Physical Chemistry A, 116 (25), 6771–6784. doi: https://doi.org/10.1021/jp303546r
19. Kovalenko, V., Kotok, V., Bolotin, O. (2016). Definition of factors influencing on Ni(OH)2 electrochemical characteristics for supercapacitors. Eastern-European Journal of Enterprise Technologies, 5 (6 (83)), 17–22. doi: https://doi.org/10.15587/1729-4061.2016.79406
20. Hu, M., Lei, L. (2006). Effects of particle size on the electrochemical performances of a layered double hydroxide, [Ni$_4$Al(OH)$_{10}$]NO$_3$. Journal of Solid State Electrochemistry, 11 (6), 847–852. doi: https://doi.org/10.1007/s10008-006-0231-y
21. Vasserman, I. N. (1980). Himicheskoe osazhdenie iz rastvorov [Chemical precipitation from solutions]. Leningrad: Himiya, 208.
22. Bora, M. (2013). Homogeneous precipitation of nickel hydroxide powders. Iowa State University, 126. doi: https://doi.org/10.31274/rtd-180813-146
23. Tang, H. W., Wang, J. L., Chang, Z. R. (2008). Preparation and characterization of nanoscale nickel hydroxide using hydrothermal synthesis method. J. Func. Mater, 39 (3), 469–476.
24. Tang, Y., Liu, Y., Yu, S., Zhao, Y., Mu, S., Gao, F. (2014). Hydrothermal synthesis of a flower-like nano-nickel hydroxide for high performance supercapacitors. Electrochimica Acta, 123, 158–166. doi: https://doi.org/10.1016/j.electacta.2013.12.187
25. Yang, L.-X., Zhu, Y.-J., Tong, H., Liang, Z.-H., Li, L., Zhang, L. (2007). Hydrothermal synthesis of nickel hydroxide nanostructures in mixed solvents of water and alcohol. Journal of Solid State Chemistry, 180 (7), 2095–2101. doi: https://doi.org/10.1016/j.jssc.2007.05.009
26. Cui, H. L., Zhang, M. L. (2009). Synthesis of flower-like nickel hydroxide by ionic liquids-assisted. J. Yanan. Univ., 28 (2), 76–83.
27. Xu, L., Ding, Y.-S., Chen, C.-H., Zhao, L., Rimkus, C., Joesten, R., Suib, S. L. (2008). 3D Flowerlike α-Nickel Hydroxide with Enhanced Electrochemical Activity Synthesized by Microwave-Assisted Hydrothermal Method. Chemistry of Materials, 20 (1), 308–316. doi: https://doi.org/10.1021/cm702207w
28. Córdoba de Torresi, S. I., Provazi, K., Malta, M., Torresi, R. M. (2001). Effect of Additives in the Stabilization of the α Phase of Ni(OH)[sub 2] Electrodes. Journal of The Electrochemical Society, 148 (10), A1179. doi: https://doi.org/10.1149/1.1403731
29. Kotok, V., Kovalenko, V., Malyshev, V. (2017). Comparison of oxygen evolution parameters on different types of nickel hydroxide. Eastern-European Journal of Enterprise Technologies, 5 (12 (89)), 12–19. doi: https://doi.org/10.15587/1729-4061.2017.109770
30. Oliva, P., Leonardi, J., Laurent, J. F., Delmas, C., Braconnier, J. J., Figlarz, M. et. al. (1982). Review of the structure and the electrochemistry of nickel hydroxides and oxy-hydroxides. Journal of Power Sources, 8 (2), 229–255. doi: https://doi.org/10.1016/0378-7753(82)80057-8
31. Kotok, V., Kovalenko, V. (2017). Electrochromism of Ni(OH)$_2$ films obtained by cathode template method with addition of Al, Zn, Co ions. Eastern-European Journal of Enterprise Technologies, 3 (12 (87)), 38–43. doi: https://doi.org/10.15587/1729-4061.2017.103010

32. Vlasova, E., Kovalenko, V., Kotok, V., Vlasov, S., Sukhyy, K. (2017). A study of the influence of additives on the process of formation and corrosive properties of tripolyphosphate coatings on steel. Eastern-European Journal of Enterprise Technologies, 5 (12 (89)), 45–51. doi: https://doi.org/10.15587/1729-4061.2017.111977
33. Kotok, V., Kovalenko, V. (2017). The properties investigation of the faradaic supercapacitor electrode formed on foamed nickel substrate with polyvinyl alcohol using. Eastern-European Journal of Enterprise Technologies, 4 (12 (88)), 31–37. doi: https://doi.org/10.15587/1729-4061.2017.108839
34. Burmistr, M. V., Boiko, V. S., Lipko, E. O., Gerasimenko, K. O., Gomza, Y. P., Vesnin, R. L. et. al. (2014). Antifriction and Construction Materials Based on Modified Phenol-Formaldehyde Resins Reinforced with Mineral and Synthetic Fibrous Fillers. Mechanics of Composite Materials, 50 (2), 213–222. doi: https://doi.org/10.1007/s11029-014-9408-0
35. Kovalenko, V., Kotok, V. (2018). Influence of ultrasound and template on the properties of nickel hydroxide as an active substance of supercapacitors. Eastern-European Journal of Enterprise Technologies, 3 (12 (93)), 32–39. doi: https://doi.org/10.15587/1729-4061.2018.133548
36. Mehdizadeh, R., Sanati, S., Saghatforoush, L. A. (2013). Effect of PEG6000 on the morphology the β-$Ni(OH)_2$ nanostructures: solvothermal synthesis, characterization, and formation mechanism. Research on Chemical Intermediates, 41 (4), 2071–2079. doi: https://doi.org/10.1007/s11164-013-1332-8
37. Ecsedi, Z., Lazău, I., Păcurariu, C. (2007). Synthesis of mesoporous alumina using polyvinyl alcohol template as porosity control additive. Processing and Application of Ceramics, 1 (1-2), 5–9. doi: https://doi.org/10.2298/pac0702005e
38. Pon-On, W., Meejoo, S., Tang, I.-M. (2008). Formation of hydroxyapatite crystallites using organic template of polyvinyl alcohol (PVA) and sodium dodecyl sulfate (SDS). Materials Chemistry and Physics, 112 (2), 453–460. doi: https://doi.org/10.1016/j.matchemphys.2008.05.082
39. Miyake, K., Hirota, Y., Uchida, Y., Nishiyama, N. (2016). Synthesis of mesoporous MFI zeolite using PVA as a secondary template. Journal of Porous Materials, 23 (5), 1395–1399. doi: https://doi.org/10.1007/s10934-016-0199-7
40. Wanchanthu, R., Thapol, A. (2011). The Kinetic Study of Methylene Blue Adsorption over MgO from PVA Template Preparation. Journal of Environmental Science and Technology, 4 (5), 552–559. doi: https://doi.org/10.3923/jest.2011.552.559
41. Kotok, V. A., Malyshev, V. V., Solovov, V. A., Kovalenko, V. L. (2017). Soft Electrochemical Etching of FTO-Coated Glass for Use in $Ni(OH)_2$-Based Electrochromic Devices. ECS Journal of Solid State Science and Technology, 6 (12), P772–P777. doi: https://doi.org/10.1149/2.0071712jss
42. Tan, Y., Srinivasan, S., Choi, K.-S. (2005). Electrochemical Deposition of Mesoporous Nickel Hydroxide Films from Dilute Surfactant Solutions. Journal of the American Chemical Society, 127 (10), 3596–3604. doi: https://doi.org/10.1021/ja0434329
43. Kotok, V., Kovalenko, V. (2018). A study of multilayered electrochromic platings based on nickel and cobalt hydroxides. Eastern-European Journal of Enterprise Technologies, 1 (12 (91)), 29–35. doi: https://doi.org/10.15587/1729-4061.2018.121679
44. Parkhomchuk, E. V., Sashkina, K. A., Rudina, N. A., Kulikovskaya, N. A., Parmon, V. N. (2013). Template synthesis of 3D-structured macroporous oxides and hierarchical zeolites. Catalysis in Industry, 5 (1), 80–89. doi: https://doi.org/10.1134/s2070050412040150
45. Gu, W., Liao, L. S., Cai, S. D., Zhou, D. Y., Jin, Z. M., Shi, X. B., Lei, Y. L. (2012). Adhesive modification of indium–tin-oxide surface for template attachment for deposition of highly ordered nanostructure arrays. Applied Surface Science, 258 (20), 8139–8145. doi: https://doi.org/10.1016/j.apsusc.2012.05.009
46. Kovalenko, V., Kotok, V. (2017). Study of the influence of the template concentration under homogeneous precepitation on the properties of $Ni(OH)_2$ for supercapacitors. Eastern-European Journal of Enterprise Technologies, 4 (6 (88)), 17–22. doi: https://doi.org/10.15587/1729-4061.2017.106813
47. Ivanov, K. V., Alekseeva, O. V., Kraev, A. S., Agafonov, A. V. (2019). Template-Free Synthesis and Properties of Mesoporous Calcium Titanate. Protection of Metals and Physical Chemistry of Surfaces, 55 (4), 667–670. doi: https://doi.org/10.1134/s2070205119040063
48. Shestakova, D. O., Sashkina, K. A., Parkhomchuk, E. V. (2019). Template-Free Synthesis of Hierarchical Zeolite ZSM-5. Petroleum Chemistry, 59 (8), 838–844. doi: http://doi.org/10.1134/S0965544119080188
49. Bhat, K. S., Nagaraja, H. S. (2019). Morphology-dependent electrochemical performances of nickel hydroxide nanostructures. Bulletin of Materials Science, 42 (6). doi: https://doi.org/10.1007/s12034-019-1951-9
50. Wang, R.-N., Li, Q.-Y., Wang, Z., Wei, Q., Nie, Z.-R. (2008). Synthesis of nickel hydroxide flower-like microspheres by template-free liquid process. Chemical Journal of Chinese Universities -Chinese Edition, 29 (1), 18–22.
51. Hadden, J. H. L., Ryan, M. P., Riley, D. J. (2019). Examining the charging behaviour of nickel hydroxide nanomaterials. Electrochemistry Communications, 101, 47–51. doi: https://doi.org/10.1016/j.elecom.2019.02.012
52. Kovalenko, V., Kotok, V. (2018). Synthesis of $Ni(OH)_2$ by template homogeneous precipitation for application in the binder-free electrode of supercapacitor. Eastern-European Journal of Enterprise Technologies, 4 (12 (94)), 29–35. doi: https://doi.org/10.15587/1729-4061.2018.140899
53. Kotok, V., Kovalenko, V. (2017). Optimization of nickel hydroxide electrode of the hybrid supercapacitor. Eastern-European Journal of Enterprise Technologies, 1 (6 (85)), 4–9. doi: https://doi.org/10.15587/1729-4061.2017.90810
54. Kovalenko, V., Kotok, V., Kovalenko, I. (2018). Activation of the nickel foam as a current collector for application in supercapacitors. Eastern-European Journal of Enterprise Technologies, 3 (12 (93)), 56–62. doi: https://doi.org/10.15587/1729-4061.2018.133472